

Goos-Hänchen shifts of an electromagnetic wave reflected from a chiral metamaterial slab

W. T. Dong¹, Lei Gao^{1,*}, and C.W. Qiu^{2,3}

¹ Jiangsu Key Laboratory of Thin Films, School of Physical Science and Technology, Soochow University, Suzhou 215006, China

² Department of Electrical and Computer Engineering, National University of Singapore, 4 Engineering Drive 3, Singapore 117576, Singapore

³ Research Laboratory of Electronics, Massachusetts Institute of Technology, 77 Mass. Avenue, Cambridge, MA 02139, USA. EMAIL: CWQ@MIT.EDU

* leigao@suda.edu.cn

Abstract: Applying Artmann's formula to the TE-polarized incident waves, we theoretically show that the Goos-Hänchen (GH) shifts near the angle of the pseudo-Brewster dip of the reflection from a slab of chiral metamaterial can be greatly enhanced. The GH shifts are observed for both parallel and perpendicular components of the reflected field. In addition, it is found that the GH shifts depend not only on the slab thickness and the incident angle, but also on the constitutive parameters of the chiral medium. In particular, when the incident angle is close to the critical angle of total reflection for LCP wave, significant enhancement of the GH shifts can be obtained. Finally, the validity of the stationary-phase analysis is demonstrated by numerical simulations of a Gaussian-shaped beam.

© 2018 Optical Society of America

OCIS codes: (260.0260) Physical optics; (260.2110) Electromagnetic optics; (160.1585) Chiral media; (120.5700) Reflection; (160.3918) Metamaterials; (350.5500) Propagation.

References and links

1. F. Goos and H. Hänchen, "Ein neuer und fundamentaler Versuch zur Totalreflexion," *Ann. Physik.* **1**, 333-346 (1947) (in German).
2. F. Goos and H. Hänchen, "Neumessung des Strahlversetzungseffektes bei Totalreflexion," *Ann. Physik.* **5**, 251-252 (1949) (in German).
3. K. Artmann, "Berechnung der Seitenversetzung des totalreflektierten Strahles," *Ann. Physik.* **2**, 87-102 (1948) (in German).
4. R. H. Renard, "Total reflection: a new evaluation of the Goos-Hänchen shift," *J. Opt. Soc. Am.* **54**, 1190-1192 (1964), <http://www.opticsinfobase.org/abstract.cfm?URI=josa-54-10-1190>.
5. B. R. Horowitz and T. Tamir, "Lateral displacement of a light beam at a dielectric interface," *J. Opt. Soc. Am.* **61**, 586-594 (1971), <http://www.opticsinfobase.org/abstract.cfm?URI=josa-61-5-586>.
6. H. M. Lai and S. W. Chan, "Large and negative Goos-Hänchen shift near the Brewster dip on reflection from weakly absorbing media," *Opt. Lett.* **27**, 680-682 (2002), <http://www.opticsinfobase.org/abstract.cfm?URI=ol-27-9-680>.
7. J. J. Cowan and B. Anicin, "Longitudinal and transverse displacements of a bounded microwave beam at total internal reflection," *J. Opt. Soc. Am.* **67**, 1307-1311 (1977), <http://www.opticsinfobase.org/abstract.cfm?URI=josa-67-10-1307>.
8. F. Bretenaker, A. Le Floch, and L. Dutriaux, "Direct measurement of the optical Goos-Hänchen effect in lasers," *Phys. Rev. Lett.* **68**, 931-933 (1992), <http://link.aps.org/doi/10.1103/PhysRevLett.68.931>.
9. A. Haibel, G. Nimtz, and A. A. Stahlhofen, "Frustrated total reflection: The double-prism revisited," *Phys. Rev. E* **63**, 047601-047603 (2001), <http://link.aps.org/doi/10.1103/PhysRevE.63.047601>.

10. O. Emile, T. Galstyan, A. Le Floch, and F. Bretenaker, "Measurement of the nonlinear Goos-Hänchen effect for Gaussian optical beams," *Phys. Rev. Lett.* **75**, 1511-1513 (1995), <http://link.aps.org/doi/10.1103/PhysRevLett.75.1511>.
11. B. M. Jost, A.-A. R. Al-Rashed, and B. E. A. Saleh, "Observation of the Goos-Hänchen effect in a phase-conjugate mirror," *Phys. Rev. Lett.* **81**, 2233-2235 (1998), <http://link.aps.org/doi/10.1103/PhysRevLett.81.2233>.
12. A. Madrazo, M. Nieto-Veperinas, "Detection of subwavelength Goos-Hänchen shifts from near-field intensities: a numerical simulation," *Opt. Lett.* **20**, 2445-2447 (1995), <http://www.opticsinfobase.org/abstract.cfm?URI=ol-20-24-2445>.
13. L.-G. Wang, H. Chen, N.-H. Liu, and S.-Y. Zhu, "Negative and positive lateral shift of a light beam reflected from a grounded slab," *Opt. Lett.* **31**, 1124-1126 (2006), <http://www.opticsinfobase.org/ol/abstract.cfm?URI=ol-31-8-1124>.
14. C. F. Li, "Negative lateral shift of a light beam transmitted through a dielectric slab and interaction of boundary effects," *Phys. Rev. Lett.* **91**, 133903-133906 (2003), <http://link.aps.org/doi/10.1103/PhysRevLett.91.133903>.
15. Y. Yan, X. Chen, and C. F. Li, "Large and negative lateral displacement in an active dielectric slab configuration," *Phys. Lett. A* **361**, 178-181 (2007), <http://dx.doi.org/10.1016/j.physleta.2006.09.023>.
16. H. Huang, Y. Fan, F. M. Kong, B.-I. Wu, and J. A. Kong, "Influence of external magnetic field on a symmetrical gyrotropic slab in terms of Goos-Hänchen shifts," *Progress In Electromagnetics Research, PIER* **82**, 137-150 (2008), <http://dx.doi:10.2528/PIER08022605>.
17. P. T. Leung, C. W. Chen, and H. P. Chiang, "Large negative Goos-Hänchen shift at metal surfaces," *Opt. Comm.*, **276**, 206-208 (2007), <http://dx.doi.org/10.1016/j.optcom.2007.04.019>.
18. M. Merano, A. Aiello, G. W. 't Hooft, M. P. van Exter, E. R. Eliel, and J. P. Woerdman, "Observation of Goos-Hänchen shifts in metallic reflection," *Opt. Exp.* **15**, 15928-15934 (2007), <http://www.opticsinfobase.org/abstract.cfm?URI=oe-15-24-15928>.
19. D. J. Hoppe, and Y. Rahmat-Samii, "Gaussian Beam reflection at a dielectric-chiral interface," *J. Electromagn. Waves Appl.* **6**, 603-624 (1992).
20. R. A. Depine, N. E. Bonomo, "Goos-Hänchen lateral shift for Gaussian Beams reflected at achiral-chiral interfaces," *Optik* **103**, 37-41 (1996).
21. W. J. Wild, and C. L. Giles, "Goos-Hänchen shifts from absorbing media," *Phys. Rev. A* **25**, 2099-2101 (1982), <http://link.aps.org/doi/10.1103/PhysRevA.25.2099>.
22. E. Pfléghaar, A. Marseille, and A. Weis, "Quantitative Investigation of the Effect of Resonant Absorbers on the Goos-Hänchen Shift," *Phys. Rev. Lett.* **70**, 2281-2284 (1993), <http://link.aps.org/doi/10.1103/PhysRevLett.70.2281>.
23. T. Tamir, and H. L. Bertoni, "Lateral displacement of optical beams at multilayered and periodic structures," *J. Opt. Soc. Am* **61**, 1397-1413 (1971), <http://www.opticsinfobase.org/abstract.cfm?URI=josa-61-10-1397>.
24. D. Felbacq, A. Moreau, and R. Smaï, "Goos-Hänchen effect in the gaps of photonic crystals," *Opt. Lett.* **28**, 1633-1635 (2003), <http://www.opticsinfobase.org/abstract.cfm?URI=ol-28-18-1633>.
25. P. R. Berman, "Goos-Hänchen shift in negatively refractive media," *Phys. Rev. E* **66**, 0676031-0676033 (2002), <http://link.aps.org/doi/10.1103/PhysRevE.66.067603>.
26. J. A. Kong, B.-L. Wu, and Y. Zhang, "Lateral displacement of a Gaussian beam reflected from a grounded slab with negative permittivity and permeability," *Appl. Phys. Lett.* **80**, 2084-2086 (2002), <http://link.aip.org/link/?APPLAB/80/2084/1>.
27. A. Lakhtakia, "On planewave remittances and Goos-Hänchen shifts of planar slabs with negative real permittivity and permeability," *Electromagnetics* **23**, 71-75 (2003).
28. D.-K. Qing and G. Chen, "Goos-Hänchen shifts at the interfaces between left- and right-handed media," *Opt. Lett.* **29**, 872-874 (2004), <http://www.opticsinfobase.org/abstract.cfm?URI=ol-29-8-872>.
29. X. Chen and C.-F. Li, "Lateral shift of the transmitted light beam through a left-handed slab," *Phys. Rev. E* **69**, 0666171-0666176 (2004), <http://link.aps.org/doi/10.1103/PhysRevE.69.066617>.
30. Y. Xiang, X. Dai, and S. Wen, "Negative and positive Goos-Hänchen shifts of a light beam transmitted from an indefinite medium slab," *Appl. Phys. A* **87**, 285-290 (2007), <http://www.springerlink.com/content/g22028831038r267/>.
31. D. R. Pendry, "A Chiral Route to Negative Refraction," *Science* **306**, 1353-1355 (2004), <http://www.sciencemag.org/cgi/content/abstract/306/5700/1353>.
32. S. Tretyakov, I. Nefedov, A. Sihvola, S. Maslovski, and C. Simovski, "Waves and Energy in Chiral Nihility," *J. Electromagn. Waves Appl.* **17**, 695-706 (2003).
33. C.-W. Qiu, N. Burokur, S. Zouhdi, and L. W. Li, "Chiral nihility effects on energy flow in chiral materials," *J. Opt. Soc. Am. A*, **25**, 53-63 (2008), <http://www.opticsinfobase.org/abstract.cfm?URI=josaa-25-1-55>.
34. C.-W. Qiu, H. Y. Yao, L. W. Li, S. Zouhdi, and T. S. Yeo, "Backward waves in magnetoelectrically chiral media: Propagation, impedance and negative refraction," *Phys. Rev. B*, **75**, 155120 (2007), <http://dx.doi.org/10.1103/PhysRevB.75.155120>.
35. W. T. Dong and L. Gao, "Negative refraction in chiral composite materials," *J. Appl. Phys.* **104**, 0235371-0235374 (2008), <http://link.aip.org/link/?JAPIAU/104/023537/1>.
36. W. T. Dong, L. Gao, and C. W. Qiu, "Goos-Hänchen shift at the surface of chiral negative refractive media,"

- Progress In Electromagnetics Research, PIER **104**, 255-268 (2009).
37. I. V. Lindell, A. H. Sihvola, S. A. Tretyakov, and A. J. Viitanen, *Electromagnetic Waves in Chiral and Bi-isotropic Media*, (Artech House, Boston, 1994).
 38. M. P. Silverman and R. B. Sohn, "Effects of circular birefringence on light propagation and reflection," *Am. J. Phys.* **54**, 69-74 (1986), <http://dx.doi.org/10.1119/1.14745> .
 39. S. Bassiri, C. H. Papas, and N. Engheta, "Electromagnetic wave propagation through a dielectric-chiral interface and through a chiral slab," *J. Opt. Soc. Am. A* **5**, 1450-1459 (1988), <http://www.opticsinfobase.org/abstract.cfm?URI=josaa-5-9-1450> .
 40. C. W. Hsue and T. Tamir, "Lateral displacement and distortion of beams incident upon a transmitting-layer configuration," *J. Opt. Soc. Am. A* **2**, 978-987 (1985), <http://www.opticsinfobase.org/abstract.cfm?URI=josaa-2-6-978> .
 41. C. F. Li and Q. Wang, "Prediction of simultaneously large and opposite generalized Goos-Hänchen shifts for TE and TM light beams in an asymmetric double-prism configuration," *Phys. Rev. E* **69**, 055601 (2004), <http://link.aps.org/doi/10.1103/PhysRevE.69.055601> .
 42. Y. Tamayama, T. Nakanishi, K. Sugiyama, and M. Kitano, "An invisible medium for circularly polarized electromagnetic waves", *Optics Express* **16**, 20869-20875 (2008), <http://www.opticsinfobase.org/oe/abstract.cfm?URI=oe-16-25-20869> .
-

1. Introduction

The Goos-Hänchen (GH) effect [1, 2], which usually refers to the lateral shift of the totally internal reflected from the position predicted by geometrical optics, has been widely analyzed both theoretically [3, 4, 5, 6] and experimentally [7, 8, 9]. This phenomenon has already been extended to many fields such as acoustics, surface optics, nonlinear optics, and quantum mechanics [10, 11]. Furthermore, with the development of near-field scanning optical microscopy and lithography [12], the importance of the GH shift has been paid more and more attention. For instance, the GH shifts were found to be large positive or negative for both reflected and transmitted beams in different media or structures, such as dielectric slabs [13, 14, 15, 16], metal surfaces [17, 18], dielectric-chiral surface [19, 20], absorptive media [21, 22], multilayered structures [23] and photonic crystals [24]. Recently, the GH shift associated with left-handed material has been extensively studied [25, 26, 27, 28, 29, 30] owing to its very unusual properties. On the other hand, since Pendry proposed the Swiss roll structure to achieve a chiral medium with negative refraction [31], negative chiral medium has been receiving great interest [32, 33, 34, 35]. In [36], we have discussed the GH shift of electromagnetic waves incident from an ordinary medium into negative chiral medium half space. But, the thickness of chiral metamaterial is always finite, and the properties of the GH shift and the reflection or transmission will strongly depend on the thickness. Therefore, it is worth discussing the effect of the thickness of the chiral metamaterial on the GH shift and the contribution of the thickness and the incident angle to the GH shift together. This is the main purpose of the present paper.

In this paper, we study the GH shifts of the reflected waves from a chiral metamaterial slab. We predict that the GH shift near the angle of the pseudo-Brewster dip from such a slab can be large, and both positive and negative lateral shifts are possible. It is also shown that the GH shift depends on the thickness of the slab, the incident angle of the wave and the constitutive parameters of the chiral medium. Finally, numerical simulations for a Gaussian-shaped beam have been performed to confirm the validity of theoretical results. Here, only perpendicularly (TE) polarized incident wave is discussed below, and the results for parallel (TM) polarized incident wave can be easily obtained in the same way.

2. Formulation

The configuration for the chiral slab in a vacuum is shown in Fig. 1. We assume that a linearly polarized wave propagating in a homogeneous isotropic dielectric medium is incident at an angle θ_i upon the surface of a chiral slab with the thickness d . The constitutive relations of the

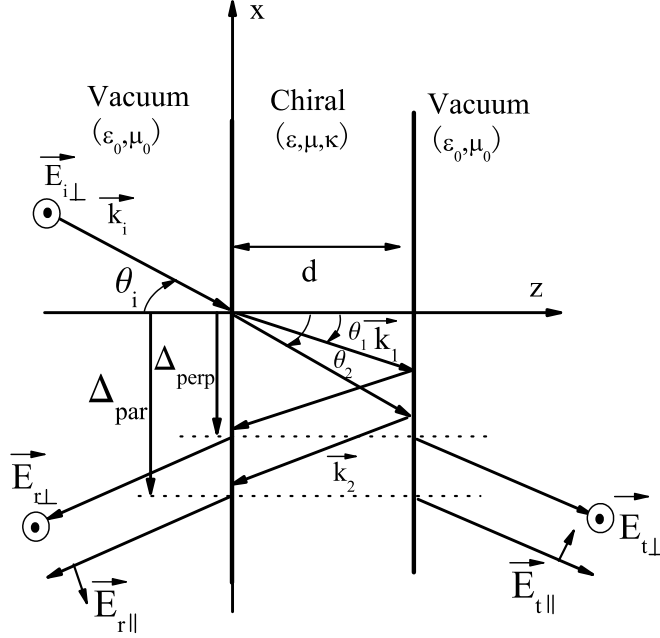


Fig. 1. Schematic diagram of a light beam propagating through the chiral slab placed in free space.

chiral slab are defined by [37]

$$\mathbf{D} = \varepsilon \varepsilon_0 \mathbf{E} - i\kappa \sqrt{\varepsilon_0 \mu_0} \mathbf{H}, \quad (1)$$

$$\mathbf{B} = \mu \mu_0 \mathbf{H} + i\kappa \sqrt{\varepsilon_0 \mu_0} \mathbf{E}, \quad (2)$$

where κ is the chirality parameter (assumed to be positive in this paper), ε and μ are the relative permittivity and permeability of the chiral medium, respectively (ε_0 and μ_0 are the permittivity and permeability in vacuum). For simplicity, a monochromatic time-harmonic variation $\exp(i\omega t)$ is assumed throughout this paper, but omitted. It is seen that two interfaces of the chiral slab are located at $z = 0$ and $z = d$.

The incident electric and magnetic fields of an incident TE wave can be written as

$$\mathbf{E}_i = E_0 \hat{y} \exp[ik_i(-\cos \theta_i z + \sin \theta_i x)], \quad (3)$$

$$\mathbf{H}_i = \sqrt{\frac{\epsilon_0}{\mu_0}} E_0 (-\cos \theta_i \hat{x} - \sin \theta_i \hat{z}) \exp[ik_i (-\cos \theta_i z + \sin \theta_i x)], \quad (4)$$

where $k_i = k_0 \equiv \omega \sqrt{\epsilon_0 \mu_0}$ is the wave number in the air. In a chiral material, an electric or magnetic excitation will produce both the electric and magnetic polarizations simultaneously [38, 39]. Therefore the reflected wave must be a combination of the perpendicular and parallel components in order to satisfy the boundary conditions. According to the propagation direction of the reflected wave, the electric and magnetic fields are expressed as

$$\mathbf{E}_r = E_0 [R_{11} \hat{y} + R_{21} \sin \theta_r \hat{z} - R_{21} \cos \theta_r \hat{x}] \exp[ik_r (\cos \theta_r z + \sin \theta_r x)], \quad (5)$$

$$\mathbf{H}_r = \sqrt{\frac{\epsilon_0}{\mu_0}} E_0 [R_{21} \hat{y} + R_{11} \cos \theta_r \hat{x} - R_{11} \sin \theta_r \hat{z}] \exp[ik_r (\cos \theta_r z + \sin \theta_r x)], \quad (6)$$

where θ_r is the reflected angle, $k_r = k_i$ is the wave number of the reflected wave, R_{11} and R_{21} are the coefficients associated with perpendicular and parallel components of the reflected wave, respectively.

Inside the chiral slab, there are two modes of propagation: a right-circularly polarized (RCP) wave at phase velocity ω/k_1 and a left-circularly polarized (LCP) wave at phase velocity ω/k_2 . The wave numbers k_1 and k_2 have the form [37]

$$k_{1,2} = k_0 (\sqrt{\epsilon \mu} \pm \kappa). \quad (7)$$

Then, the refractive indices of the two eigen-waves in the chiral medium are thus given as

$$n_{1,2} = \sqrt{\epsilon \mu} \pm \kappa. \quad (8)$$

Recent studies have shown that $\kappa > \sqrt{\epsilon \mu}$ can occur at least at or near the resonant frequency of the permittivity of a chiral medium (called chiral nihility [32]), and then backward wave will occur to one of the two circularly polarized eigen-waves, making negative refraction in the chiral medium possible. When $\kappa > \sqrt{\epsilon \mu}$, the refraction index $n_1 \equiv \sqrt{\epsilon \mu} + \kappa$ will still be positive, but the refraction index $n_2 \equiv \sqrt{\epsilon \mu} - \kappa$ will become negative. Correspondingly, negative refraction will arise for LCP wave. Based on the discussion above, in the chiral slab, it is assumed that there exist four total waves, two propagating toward the interface $z = d$ and the other two propagating toward the interface $z = 0$ (see Fig. 1). The electric and magnetic fields of these waves propagating inside the chiral medium toward the interface $z = d$ are written as

$$\mathbf{E}_c^+ = E_0 [A_1 \cos \theta_1 \hat{x} + A_1 \sin \theta_1 \hat{z} + iA_1 \hat{y}] \exp[ik_1 (-\cos \theta_1 z + \sin \theta_1 x)] \\ + E_0 [A_2 \cos \theta_2 \hat{x} + A_2 \sin \theta_2 \hat{z} - iA_2 \hat{y}] \exp[ik_2 (-\cos \theta_2 z + \sin \theta_2 x)], \quad (9)$$

$$\mathbf{H}_c^+ = i\eta^{-1} E_0 [A_1 \cos \theta_1 \hat{x} + A_1 \sin \theta_1 \hat{z} + iA_1 \hat{y}] \exp[ik_1 (-\cos \theta_1 z + \sin \theta_1 x)] \\ - i\eta^{-1} E_0 [A_2 \cos \theta_2 \hat{x} + A_2 \sin \theta_2 \hat{z} - iA_2 \hat{y}] \exp[ik_2 (-\cos \theta_2 z + \sin \theta_2 x)]. \quad (10)$$

The total electromagnetic fields of the other two waves propagating inside the chiral medium toward the interface $z = 0$ are expressed as

$$\mathbf{E}_c^- = E_0 [-B_1 \cos \theta_1 \hat{x} + B_1 \sin \theta_1 \hat{z} + iB_1 \hat{y}] \exp[ik_1 (\cos \theta_1 z + \sin \theta_1 x)] \\ + E_0 [-B_2 \cos \theta_2 \hat{x} + B_2 \sin \theta_2 \hat{z} - iB_2 \hat{y}] \exp[ik_2 (\cos \theta_2 z + \sin \theta_2 x)], \quad (11)$$

$$\mathbf{H}_c^- = i\eta^{-1} E_0 [-B_1 \cos \theta_1 \hat{x} + B_1 \sin \theta_1 \hat{z} + iB_1 \hat{y}] \exp[ik_1 (\cos \theta_1 z + \sin \theta_1 x)] \\ - i\eta^{-1} E_0 [-B_2 \cos \theta_2 \hat{x} + B_2 \sin \theta_2 \hat{z} - iB_2 \hat{y}] \exp[ik_2 (\cos \theta_2 z + \sin \theta_2 x)], \quad (12)$$

where $\eta = \sqrt{\mu/\epsilon}$ is the wave impedance of the chiral medium, $A_{1,2}$ and $B_{1,2}$ are the transmitted coefficients, and $\theta_{1,2}$ denote the refracted angles of the two eigen-waves in the chiral slab, respectively.

Outside the slab ($z > d$), the total transmitted wave can be expressed as

$$\mathbf{E}_t = E_0[T_{11}\hat{y} + T_{21}\sin\theta_t\hat{z} + T_{21}\cos\theta_t\hat{x}] \exp[ik_t(-\cos\theta_t z + \sin\theta_t x)], \quad (13)$$

$$\mathbf{H}_t = \sqrt{\frac{\epsilon_0}{\mu_0}} E_0[T_{11}\hat{y} - T_{21}\sin\theta_t\hat{z} - T_{21}\cos\theta_t\hat{x}] \exp[ik_t(-\cos\theta_t z + \sin\theta_t x)], \quad (14)$$

where $k_t = k_i$, θ_t is the transmitted angle, T_{11} and T_{21} are coefficients associated with perpendicular and parallel components of the transmitted wave in the air, respectively.

The coefficients R_{11} , R_{21} , $A_{1,2}$, $B_{1,2}$, T_{11} and T_{21} can be determined by matching the boundary conditions at two interfaces $z = 0$ and $z = d$, and the following matrix can be obtained:

$$\begin{pmatrix} [\Psi]_{11} & [\Psi]_{12} \\ [\Psi]_{21} & [\Psi]_{22} \end{pmatrix} \cdot \begin{pmatrix} R_{11} \\ R_{21} \\ T_{11} \\ T_{21} \end{pmatrix} = \begin{pmatrix} -i\eta \cos\theta_i + i \cos\theta_1 \\ i\eta \cos\theta_i + i \cos\theta_1 \\ i\eta \cos\theta_i - i \cos\theta_2 \\ -i\eta \cos\theta_i - i \cos\theta_2 \end{pmatrix}. \quad (15)$$

where

$$[\Psi]_{11} = \begin{pmatrix} -i(\eta \cos\theta_i + \cos\theta_1) & -\cos\theta_i - \eta \cos\theta_1 \\ i(\eta \cos\theta_i - \cos\theta_1) & \cos\theta_i - \eta \cos\theta_1 \end{pmatrix} \quad (16)$$

$$[\Psi]_{21} = \begin{pmatrix} i(\eta \cos\theta_i + \cos\theta_2) & -\cos\theta_i - \eta \cos\theta_2 \\ -i(\eta \cos\theta_i - \cos\theta_2) & \cos\theta_i - \eta \cos\theta_2 \end{pmatrix} \quad (17)$$

$$[\Psi]_{12} = \begin{pmatrix} i(-\eta \cos\theta_i + \cos\theta_1)e^{-i(k_{iz}-k_{1z})d} & (-\cos\theta_i + \eta \cos\theta_1)e^{-i(k_{iz}-k_{1z})d} \\ i(\eta \cos\theta_i + \cos\theta_1)e^{-i(k_{iz}+k_{1z})d} & (\eta \cos\theta_1 + \cos\theta_i)e^{-i(k_{iz}+k_{1z})d} \end{pmatrix} \quad (18)$$

$$[\Psi]_{22} = \begin{pmatrix} i(\eta \cos\theta_i - \cos\theta_2)e^{-i(k_{iz}-k_{2z})d} & (-\cos\theta_i + \eta \cos\theta_2)e^{-i(k_{iz}-k_{2z})d} \\ -i(\eta \cos\theta_i + \cos\theta_2)e^{-i(k_{iz}+k_{2z})d} & (\eta \cos\theta_2 + \cos\theta_i)e^{-i(k_{iz}+k_{2z})d} \end{pmatrix}. \quad (19)$$

The analytic solutions to the above matrix can be obtained after some lengthy mathematic manipulations, but the final results are too complicated to reproduce here. Now we would like to study the GH shifts of the reflected beams from a slab of negative chiral medium. It is well known that the lateral shift of the reflected beam has the definition

$$\Delta = d\Phi/dk_x, \quad (20)$$

which was proposed by Artmann using the stationary-phase method [3]. Φ is the phase difference between the reflected and incident waves. For a chiral medium, the reflected field contains both parallel and perpendicular components, these field components can to first order be represented as two separate reflected beams, each with its own magnitude and lateral shift. Then the GH lateral shifts for perpendicular component (R_{11} in Eq. (15)) and parallel component (R_{21} in Eq. (15)) of the reflected wave can be calculated by the stationary-phase approach as a function of the angle of incidence.

3. Results and discussion

In this section, numerical simulations associated with the GH lateral shifts for a negative chiral slab will be presented and compared with a conventional chiral slab.

In our calculation, we consider two types of chiral slabs: (1) a positive chiral slab (e.g., $\epsilon = 0.64$, $\mu = 1$, $\kappa = 0.4$) whose refraction indices of RCP and LCP waves are both positive, i.e., a conventional chiral slab; (2) a negative chiral slab (e.g., $\kappa = 1.4$ and the other parameters unchanged) whose refraction index of LCP wave is $n_2 = -0.6$. The working frequency here is $\omega = 2\pi \times 10$ GHz, and the thickness d of the chiral slab is 1.5λ . Figs. 2(a) and 2(b) show

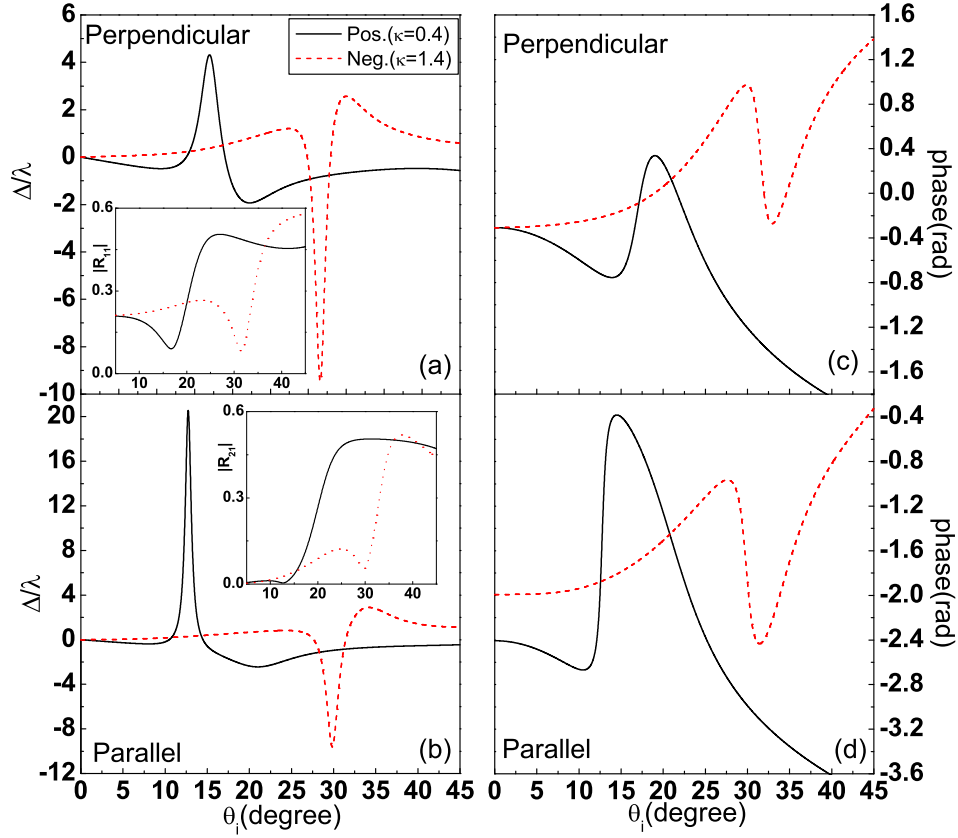


Fig. 2. The dependence of (a,b) the lateral shifts and (c,d) the phases of the reflection coefficients for (a,c) perpendicular and (b,d) parallel components on the incident angle in the presence of different chiral slabs. The insets of (a) and (b) show the absolute values of perpendicular and parallel reflection coefficients, respectively. Solid line and dashed line correspond to positive chiral slab and negative chiral slab, respectively.

the dependence of the GH shifts of the reflected beam upon the incident angle for both perpendicular and parallel components from the slab of Type-1 and Type-2. In Figs. 2(a) and 2(b), both the insets show, respectively, the absolute values of perpendicular and parallel reflection coefficients for two different types. It is easily found that there is a dip in each reflection curve, at which $|R|$ reaches the minimum (close to zero). The corresponding incident angle is defined as the pseudo-Brewster angle. From Figs. 2(a) and 2(b), we clearly see that the behaviors of the GH shifts for perpendicular and parallel components are similar, and the shift will be greatly enhanced near the angle of pseudo-Brewster dip. For the negative chiral slab, the lateral shifts of both reflected components might be large negative near the dip, and be small positive values under other incident angles. This phenomenon can be easily explained in terms of the change of phase. The phases of reflected parallel and perpendicular components as a function of the incident angle are plotted in Figs. 2(c) and 2(d) for negative and positive chiral slabs. Near the angle of the dip, the phase of reflection experiences a distinct sharp variation, which decreases

quickly for the chiral negative slab. As a result, Artmann's formula Eq. (16) leads to a large negative GH shift and small positive lateral shift. In contrast to chiral negative slab, for the positive chiral slab, both components have positive lateral shifts near the angle of dip, and then experience small negative shifts over other incident angles. The dependence of GH shifts on incident angle for negative chiral slab is opposite to that for positive chiral slab.

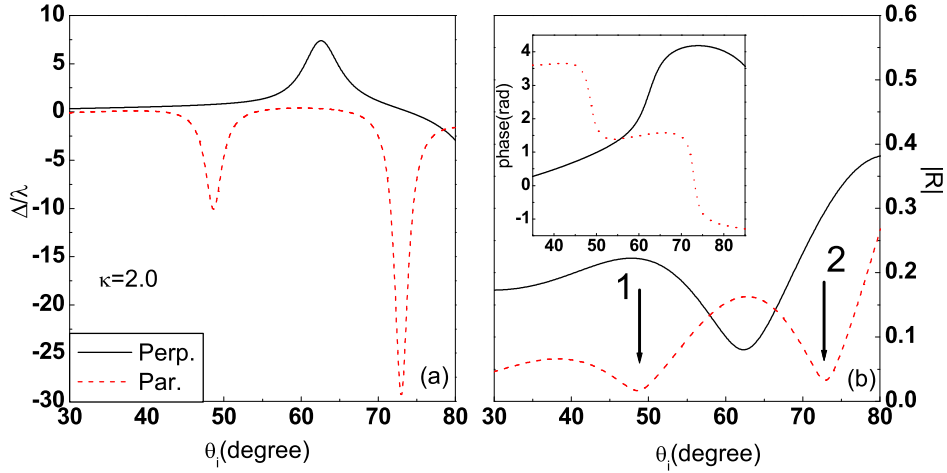


Fig. 3. (a) The dependence of the lateral shifts for reflected perpendicular and parallel components on the incident angle for a typical negative chiral slab. (b) The absolute values of perpendicular and parallel reflection coefficients. The inset of (b) is the phase of both reflection coefficients.

Figure 3 shows a typical dependence of the GH shifts of reflected perpendicular and parallel components on the incident angle from a negative chiral slab with a large chirality parameter. Assume that the chiral slab has a chirality $\kappa = 2.0$, while other parameters remain the same as before. Figure 3(b) shows the absolute values of the reflection coefficients for perpendicular and parallel components as a function of the incident angle. It can be seen that there is only one dip in the perpendicular reflection curve, at which the reflection coefficient reaches a minimum magnitude and the phase difference increases monotonically as a function of incident angle (see the inset of Fig. 3(b)). Thus the GH shift of the reflected perpendicular component has a positive peak near the angle of the dip. In contrast, there are two dips in the parallel reflection component, where the absolute values of the reflection coefficient are very close to zero. Meanwhile, from the inset of Fig. 3(b), the corresponding phase in the vicinity of these two dips monotonically decreases quickly. Therefore, it indicates that the shifts of the parallel component can be greatly enhanced to be large negative near certain angles where the phase decreases. The shift enhancement can be an order in magnitude greater than the wavelength.

In what follows, we turn to discuss the lateral shift as a function of the thickness of the slab under different incident angles. First, we consider the GH shifts of the reflected beam from a negative chiral slab. As an example, the dependence of lateral shifts on the slab thickness at different incident angles is presented in Fig. 4. The parameters are taken as follows: $\varepsilon = 0.64$, $\mu = 1$, $\kappa = 1.3$, implying that two refraction indices corresponding to RCP and LCP waves are $n_1 = 2.1$ and $n_2 = -0.5$. It is obvious that there exists a critical angle at $\theta_c = 30^\circ$ for the LCP

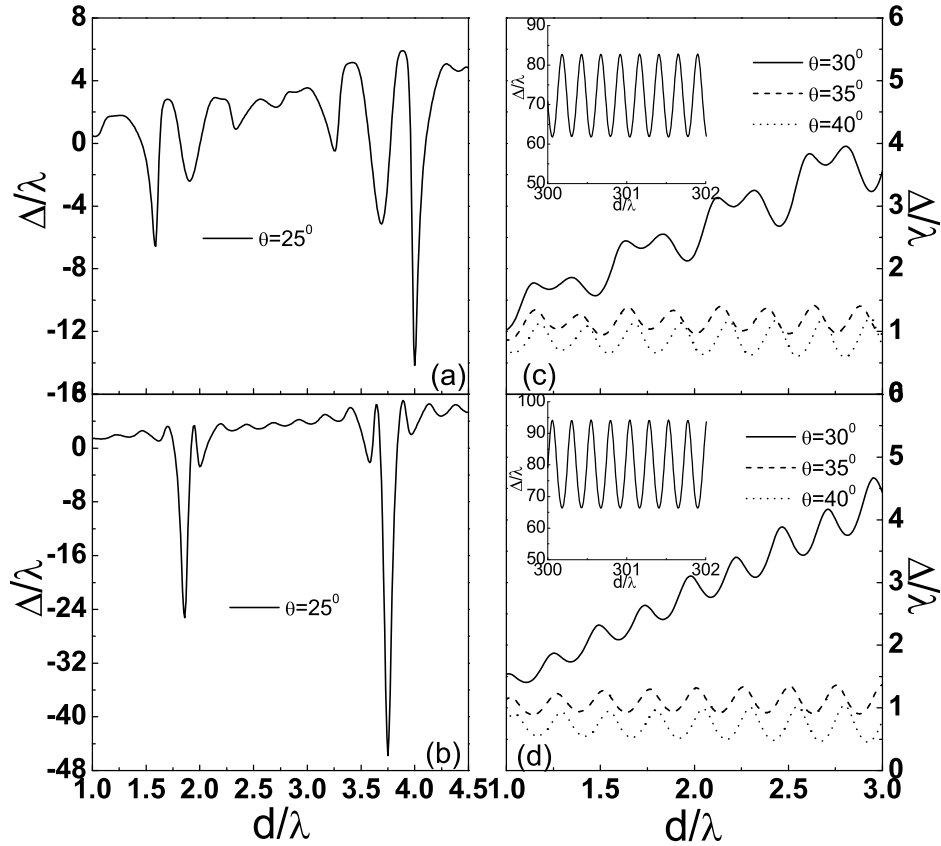


Fig. 4. The dependence of lateral shift on the thickness of the chiral negative slab for different incident angles. (a) and (c) Reflected perpendicular component; (b) and (d) Reflected parallel component.

wave, but it does not correspond to the true total reflection. Under such critical situation, only LCP wave in the chiral slab becomes evanescent wave when the incident angle exceeds this critical angle, while the RCP wave will still propagate through the chiral slab. Correspondingly, this incident angle is defined as pseudo-critical angle. However, the true total internal reflection will never arise under these parameters. In such a case, when the incident angle is smaller than the critical angle ($\theta_c = 30^\circ$), it is shown in Fig. 4(a) that the GH shift of the reflected perpendicular component could reach large negative or positive values, but there never exists any periodic fluctuation of the lateral shift with respect to the thickness. Similar phenomenon can be found from the shift of the parallel component (see Fig. 4(b)). Their large negative enhancement of the lateral shifts correspond to the dips of the reflection coefficients, which follows previous discussions. However, when the incident angle is equal to the critical angle of the LCP wave, as shown in Figs. 4(c) and 4(d), the lateral shifts of both reflected components are always positive and increasing with respect to the thickness of the slab. This can be explained by the fluctuation of the reflection coefficient with the slab thickness. However when the slab is

much thicker, the strong fluctuation of GH shift can be attained, as shown in the insets of Fig. 4. And when the incident angle further increases above the pseudo-Critical angle, the small fluctuation of the lateral shift against the slab thickness is observed, as shown in Figs. 4(c) and 4(d).

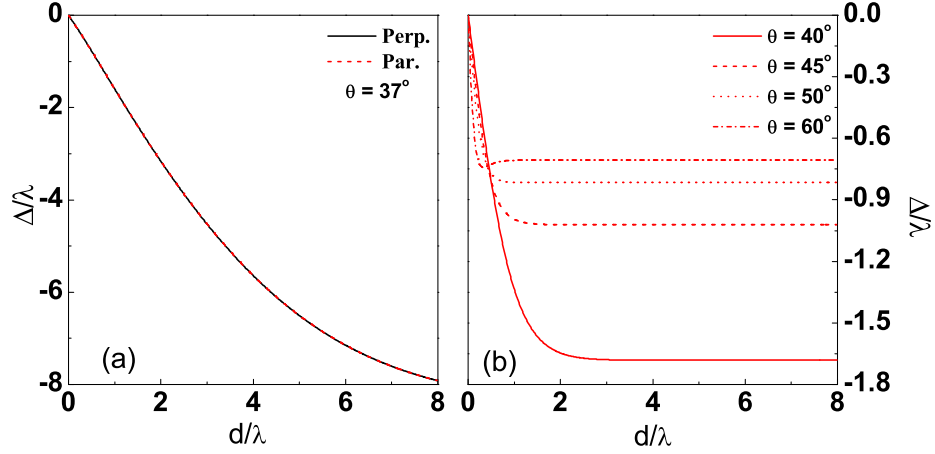


Fig. 5. Dependence of the GH shift on the thickness of an invisible medium slab for different incident angles. $\varepsilon = 0.8$, $\mu = 0.8$, and $\kappa = 0.2$.

Apart from the above-mentioned the GH shift of the negative chiral slab, we also consider the lateral shift of the other chiral metamaterial slab. Here, we set the parameters of the chiral medium as $\varepsilon = 0.8$, $\mu = 0.8$, and $\kappa = 0.2$. In this case, the wavenumber matching condition $k_1 = k_0$ and the wave impedance matching condition $\eta = \eta_0$ are satisfied simultaneously, the RCP wave is transmitted straight through the chiral medium without either reflection or refraction at any incident angle. This medium is invisible for RCP wave [42]. While the LCP wave can be refracted and reflected, or totally reflected. This unusual phenomenon can be physically understood as a destructive interference of electric and magnetic responses, due to the mixing through the chirality parameter. For $k_2 = 0.6k_0$, Snell's equation for LCP wave is expressed as $\sin \theta_1 = 0.6 \sin \theta_2$, so the critical angle for LCP wave is $\theta_c = \arcsin 0.6 \simeq 37^\circ$. Therefore, LCP wave is totally reflected with the incident angle greater than 37° . This implies that we can divide the incident wave into LCP and RCP waves. The property of GH shifts for this case is shown in Fig. 5. Fig. 5(a) shows the perpendicular and the parallel reflected GH shifts as a function of the slab thickness when the incident angle is equal to the critical angle of the LCP wave ($\theta_c = 37^\circ$). Calculation under these conditions shows that both reflected components have the same GH shift. This is because the reflected wave only has LCP wave, and the RCP wave contributes to the transmitted wave. Hence the perpendicular and the parallel reflection coefficients have the same absolute value, while their phases are different. From Fig. 5, it is straightforward to see that the calculated lateral shifts for this case are negative. Moreover, when the incident angle is close to the critical angle of the LCP wave, the lateral shifts are large and increase as the slab thickness increases. While the incident angle is greater than θ_c , we can see that, as the increase of the slab thickness, the lateral shifts will increase quickly and then gradually approach to an asymptotic negative value. Therefore, the GH shift for the thick slab in the present case depends

on the incident angle more than the slab thickness.

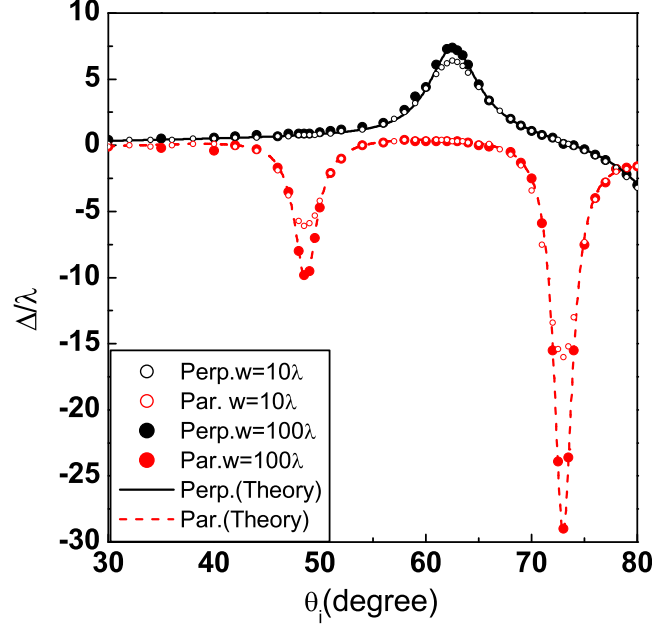


Fig. 6. Dependence of the GH shift on the incident angle. The theoretical result is shown by the line; the numerical results are shown by solid scatters (for $w_0 = 10\lambda$) and open scatters ($w_0 = 100\lambda$), all the other optical parameters are the same as in Fig. 3(a).

4. Goos-Hänchen shift of a Gaussian-shaped incident beam

To show the validity of the above stationary-phase analysis, numerical calculations are performed, which confirm our theoretical results. In the numerical simulation, an incident Gaussian-shaped beam is assumed, $E_i(x, z = 0) = \exp(-x^2/2w_x^2 + ik_{x0}x)$, which has the Fourier integral of the following form:

$$E_i(x, z = 0) = \int_{-\infty}^{\infty} A(k_x) \exp(ik_x x) dk_x \quad (21)$$

where $w_x = w_0 \sec \theta_i$, w_0 is the beam width at the waist, and the amplitude angular-spectrum distribution is Gaussian, $A(k_x) = \frac{w_x}{\sqrt{2\pi}} \exp[-\frac{w_x^2}{2}(k_x - k_{x0})^2]$. So the electric fields (E_{\perp}^r and E_{\parallel}^r) of the reflected beam, determined from the transformation of the incident beam, can be written as

$$E_{\perp}^r(x, z = 0) = \int_{-\infty}^{\infty} R_{11} A(k_x) \exp(ik_x x) dk_x, \quad (22)$$

$$E_{\parallel}^r(x, z = 0) = \int_{-\infty}^{\infty} R_{21} A(k_x) \exp(ik_x x) dk_x. \quad (23)$$

The calculated beam shift can be obtained by finding the location where $|E_{\perp}^r|_{z=0}$ or $|E_{\parallel}^r|_{z=0}$ is maximal [14].

Calculations show that the stationary-phase approximation for the GH shift is in good agreement with the numerical result. As an example, Fig. 6 shows the numerical calculation results of curves in Fig. 3(a). The incident beam width is chosen to be $w_0 = 10\lambda$ and $w_0 = 100\lambda$. For comparison, both the numerical and theoretical results are shown in Fig. 6. The peaks of the numerical shifts for the perpendicular reflected field are about 6.4λ for $w_0 = 10\lambda$ and 7.4λ for $w_0 = 100\lambda$, and for the parallel reflected field are about -6.1λ (dip I), -16λ (dip II) for $w_0 = 10\lambda$, and -9.8λ (dip I), -29.0λ (dip II) for $w_0 = 100\lambda$. The peaks of the theoretical shifts are about 7.39λ for the perpendicular field and -10.07λ (-29.32λ) for dip I (dip II) of the parallel field. It is noted that the discrepancy between theoretical and numerical results is due to the distortion of the reflected beam, especially when the waist of the incident beam is narrow [40, 41]. The further numerical simulation shows that the wider the incident beam is, the less the discrepancy is, and the closer to the stationary-phase result the numerical result is.

5. Conclusion

To summary, an investigation on the GH shifts of both reflected parallel and perpendicular components for chiral metamaterial slab has been done by using the stationary-phase approach. It shows that the GH shift of the reflected perpendicular components can be greatly enhanced to be large negative as well as positive near the dip of the reflection curve, at which $|R|$ reaches a minimum. Similar behavior will be found for the parallel component. These results obtained from the negative chiral slab are opposite to those from the conventional chiral slab. In addition, at a given incident angle, the dependence of the GH shift on the slab thickness for negative chiral slabs has also been studied. It is shown that, when the incident angle is equal to the critical angle of the LCP wave, the GH shifts of both reflected components oscillate with respect to the thickness of the slab, and its overall tendency is increasing along with the small slab thickness, while for a much thicker slab, the fluctuation of the lateral shift with the slab thickness becomes more obvious. However, greatly enhanced GH shifts for a smaller thickness slab can be obtained when the incident angle is smaller than the critical angle. Meanwhile, we calculated the GH shift of an invisible chiral medium for RCP wave. Finally, in order to demonstrate the validity of the stationary-phase approach, numerical simulations are made for a Gaussian-shaped beam. Calculation results show that the wider the waist of the incident beam is, the closer to the stationary-phase result it is.

Acknowledgments

This work was supported by the National Natural Science Foundation of China under Grant No. 10674098, the National Basic Research Program under Grant No. 2004CB719801, the Key Project in Science and Technology Innovation Cultivation Program of Soochow University, and the Natural Science of Jiangsu Province under Grant No. BK2007046.